Energy loss of slow C_{60}^+ ions during grazing scattering from a KCl(001) surface

T. Matsushita, K. Nakajima, M. Suzuki, and K. Kimura*
Department of Micro Engineering, Kyoto University, Yoshida-honmachi, Sakyo, Kyoto 606-8501, Japan
(Received 25 July 2007; published 28 September 2007)

The energy spectra of 1–3 keV C_{60}^+ ions reflected from a KCl(001) surface under grazing incidence are measured with an electrostatic spectrometer. Although both nuclear and electronic energy losses are expected to be almost completely suppressed in the grazing scattering of such extremely low energy ions ($v \sim 0.01$ a.u.) from the wide-band-gap insulator surface, we observe anomalously large energy losses ranging from ~25 eV ($\theta_i = 1°$) to ~100 eV ($\theta_i = 6°$). Fragmentation of C_{60}^+ ions via sequential C_2 loss is also observed during grazing scattering. We find a strong correlation between the energy loss and the fragmentation. From these results the observed anomalous energy losses are attributed to the internal excitations of C_{60}^+ ions.

DOI: 10.1103/PhysRevA.76.032903 PACS number(s): 79.20.Rf, 34.50.Bw, 78.30.Na, 79.60.Bm

I. INTRODUCTION

The dissipation of the kinetic energy of projectile ions in solids is one of the most fundamental phenomena in ion-solid interactions. Since the pioneering work by Bohr the stopping of energetic ions in solids has been extensively studied. The stopping is divided into two major components: nuclear stopping (binary collisions with target atoms) and electronic stopping (energy transfer to the target electrons). When cluster ions are used as projectiles, interesting aspects may arise in the stopping phenomena. One of the most interesting aspects is the interference effects between the constituent ions [1,2], which is now well understood after extensive studies. Another interesting but rarely investigated aspect is the role of the internal degrees of freedom. The kinetic energy may be transferred to the internal excitations of the cluster ion. In ion-solid collisions, however, the cluster ions are easily dissociated into fragments. Only under special conditions, the energy loss of the cluster ion can be measured without fragmentation. Susuki *et al.* measured energy losses of 10 MeV/amu H_2^+ and H_3^+ ions passing through ultrathin carbon foils without fragmentation [3,4]. The observed energy losses, however, were well explained in terms of the electronic stopping power and no clear signature of the energy loss due to the internal excitations was observed. In order to investigate the effect of the internal excitations on the energy loss, the usual energy loss mechanisms, i.e., nuclear and electrostatic stopping powers, should be suppressed.

Regarding the fragility of the cluster ions, the Buckminster fullerene ion C_{60}^+ is unusually stable against surface impacts [5,6]. Recent Monte Carlo simulations for C_{60} impact on a structureless potential wall showed that there is a threshold impact energy of ~150 eV for fragmentation of C_{60} [7]. This threshold energy corresponds to the grazing angle of incidence $\theta_i = 7°$ for 10 keV C_{60}^+, indicating that the energy loss of keV C_{60}^+ ions can be observed without fragmentation under grazing scattering. In addition, the grazing scattering provides other advantages for the investigation of the energy loss due to the internal excitations. Borisov *et al.* demonstrated that both the nuclear and electronic energy losses can be suppressed under grazing scattering of keV ions at LiF(001) [8]. The nuclear stopping power is reduced due to the channeling effect [9] and the wide band gap of LiF also suppresses the electronic excitation almost completely at slow projectile velocities ($v \leq 0.1$ a.u.) [8].

In the present paper, we measure the energy losses of 1–3 keV C_{60}^+ ions reflected from a KCl(001) surface under grazing incidence. In spite of the suppression of the nuclear and electronic stopping powers, we observe rather large energy losses, which are attributed to the internal excitations of C_{60}^+ ions.

II. EXPERIMENTAL

A single crystal of KCl was cleaved in air and mounted on a five-axis precision goniometer in an ultrahigh vacuum chamber (base pressure 2×10^{-10} Torr). The surface of KCl(001) was heated to 300 °C to prepare a clean surface [10] and kept at 250 °C during the measurements to prevent surface charging [11]. A beam of C_{60}^+ ions produced by a 10 GHz electron cyclotron resonance (ECR) ion source was collimated to less than 0.5×0.5 mm^2 after mass separation. The beam was guided into the chamber and incident on a KCl(001) surface at a grazing angle. The azimuth angle of incidence was adjusted to avoid surface axial channeling. The energy spectrum of the reflected ions was measured by a cylindrical electrostatic analyzer (CEA). The CEA was placed 100 mm downstream of the target KCl crystal and was able to rotate around the target. The measured energy resolution of the CEA was less than 0.25%.

The angular and charge state distributions of the reflected particles were also measured by a two-dimensional position-sensitive detector (2D PSD) equipped with a pair of electric field plates. The diameter of 2D-PSD was 40 mm and was placed 160 mm downstream of the target KCl crystal.

III. RESULTS AND DISCUSSION

A. Angular and charge state distributions

Figure 1 shows an example of the angular distribution of the reflected particles observed under operation of the elec-

*Corresponding author; FAX: +81-75-753-5253; kimura@kues.kyoto-u.ac.jp

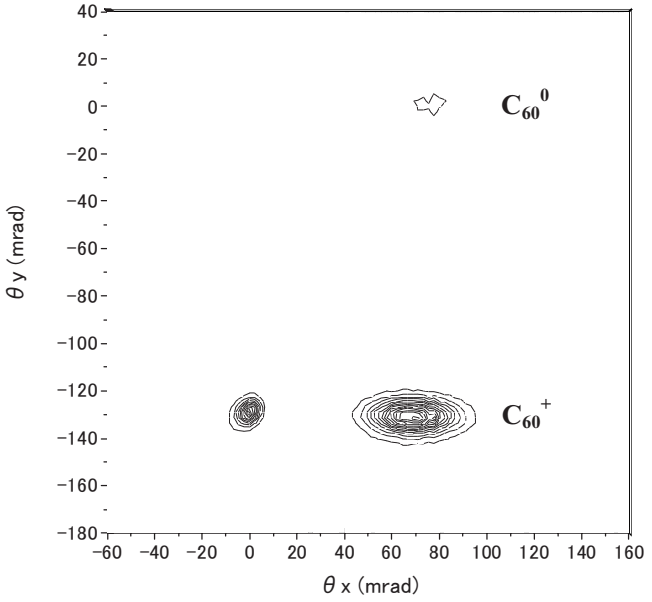

FIG. 1. Observed angular distribution of the reflected particles when 3 keV C_{60}^{+} ions are incident onto a KCl(001) surface at $\theta_i = 2°$.

tric field plates when 3 keV C_{60}^{+} ions were incident onto a KCl(001) surface at $\theta_i = 2°$. The residual incident C_{60}^{+} ions appear as a sharp peak on the lower left-hand side. The largest peak on the lower right-hand side corresponds to the reflected C_{60}^{+} ions and a small peak seen on the upper right-hand side corresponds to the reflected neutral particles. The observed neutral fraction is only ~10% in spite of the very low velocity ($v = 0.013$ a.u.). This is because the ionization energy of C_{60} (7.6 eV) locates in the band gap of KCl. As the result, both resonant and Auger neutralization processes are not allowed for slow C_{60}^{+} ions in front of a KCl(001) surface [12]. This situation is different from the scattering from metal surfaces. A recent study on the neutralization of keV $C_{60}^{+,2+}$ ions during grazing scattering from Al(001) has shown complete neutralization [13], where the energy loss associated with the charge exchange processes may not be neglected.

Figure 2 shows the observed most probable scattering angles of 3 keV C_{60}^{+} and neutral C_{60} as a function of θ_i. The dashed line indicates specular reflection. All data points of C_{60}^{+} fall on this line, indicating that the C_{60}^{+} ions are specularly reflected from KCl(001). This means that there is no dissipation of the perpendicular energy and the motion of C_{60}^{+} is governed by a continuum surface potential. This is very different from the observation of C_{60}^{+} scattering from highly oriented pyrolytic graphite (HOPG) surfaces at $\theta_i = 15°$ [14]. The C_{60}^{+} were scattered subspecularly and the observed most probable scattering angle changed from 13.5° to 5° when the incident energy was changed from 0.5 to 5 keV. This subspecular reflection was reproduced by molecular dynamics (MD) simulation and was attributed to effective deformation of the surface atomic plane during scattering. For a diamond surface, however, MD simulation showed specular reflection under analogous conditions and it was concluded that the subspecular reflection is a consequence of an HOPG structure-specific effect [14].

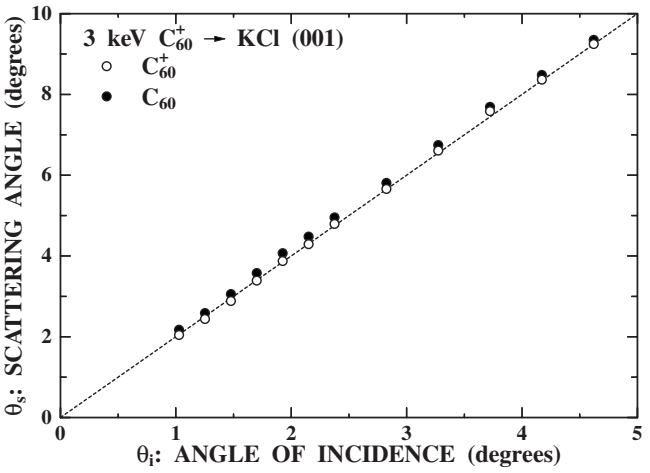

FIG. 2. Most probable scattering angle of reflected ions (closed circles) and neutral particles (open circles) when 3 keV C_{60}^{+} ions are incident onto a KCl(001) surface. The dashed line indicates specular reflection. All data points of reflected C_{60}^{+} ions fall on the dashed line while the scattering angles of the neutral particles are slightly larger than the specular angle due to the image acceleration.

Looking at Fig. 2 more closely, slight shifts of the C_{60} scattering angle toward larger angles can be seen. These angular shifts can be ascribed to the image acceleration of C_{60}^{+} [15]. The energy gain can be derived from the observed scattering angles,

$$\Delta E_g = E[\sin^2(\theta_s^0 - \theta_i) - \sin^2(\theta_s^+ - \theta_i)], \tag{1}$$

where E is the ion energy, and θ_s^+ and θ_s^0 denote the scattering angles of C_{60}^{+} and C_{60}^{0}, respectively. Because the neutralization takes place mainly near the closest approach $x_{\min}$ to the surface, the observed energy gain represents the image potential at $x_{\min}$. The closest approach distance can be estimated by

$$E \sin^2(\theta_s^0 - \theta_i) = V_0(x_{\min}), \tag{2}$$

where $V_0(x)$ is the surface continuum potential for C_{60}^{0}. Figure 3 shows the estimated image potential as a function of the distance from the surface. In this estimation, the sum of the Ziegler-Biersack-Littmark (ZBL) potentials for the constituent C atoms was used for $V_0(x)$. Recently, the image potential of C_{60}^{+} in front of a metal surface has been calculated by Wethekam *et al.* [13] by extending the method developed by Zettergren *et al.* [16]. Here, we modify their result to calculate the image potential of C_{60}^{+} in front of an insulator surface. The C_{60}^{+} is treated as a conductive sphere with a radius $R = 0.443$ nm [13]. The image potential of C_{60}^{+} at a distance r from the surface is given by

$$U_{img} = \frac{e^2}{2} \sum_{n=0}^{\infty} \mu_n \left(\frac{1}{R - \delta_n} - \frac{\varepsilon(0) - 1}{\varepsilon(0) + 1} \frac{1}{2r - R - \delta_n} \right) \Bigg/ \sum_{n=0}^{\infty} \mu_n - \frac{e^2}{2R}, \tag{3}$$

where $\varepsilon(0) = 4.85$ is the dielectric constant of KCl,

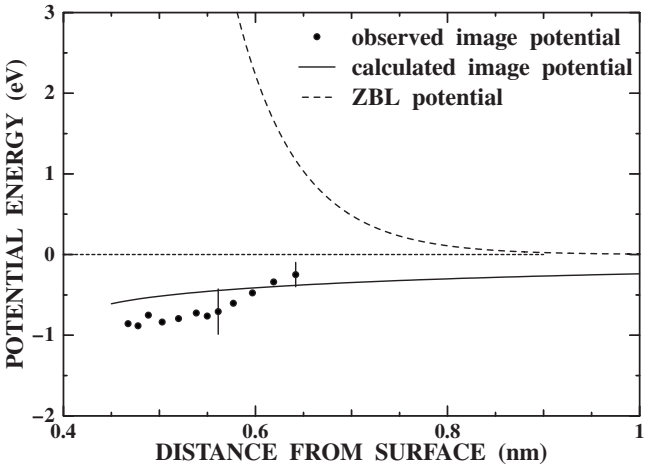

FIG. 3. Image potential of C_{60}^+ ions in front of a KCl(001) surface estimated from the observed scattering angles of C_{60}^+ and C_{60}^0. Typical experimental errors are shown. The solid line shows the calculated image potential.

$$\mu_n = \left(\frac{\varepsilon(0)-1}{\varepsilon(0)+1}\right)^{n^{n-1}} \prod_{i=0} \frac{R}{2r-\delta_i}, \tag{4}$$

and

$$\delta_{n+1} = \frac{R^2}{2r-\delta_n}, \quad \delta_0 = 0. \tag{5}$$

The calculated result roughly reproduces the observed image potential within the experimental error. In the following section, we will use both ZBL potential and the image potential given by Eqs. (3)–(5) to calculate the trajectory of C_{60}^+ ions.

B. Energy spectrum of reflected C_{60}^+

Figure 4 shows examples of the observed energy spectra of the specularly reflected 3 keV C_{60}^+. The spectrum has a sharp peak at energies slightly lower than the incident energy when θ_i is small. With increasing θ_i, the peak shifts toward lower energies and additional small peaks appear in the low energy side of the first peak. The number and the intensities of these additional peaks increase with θ_i. Figure 5 shows the observed energy losses of these peaks as a function of θ_i. These peaks are almost equally separated by ~106 eV irrespective of θ_i. Such a multipeak structure might be attributed to either *skipping motion* [17] or *subsurface channeling* [18]. In the case of the skipping motion, however, the energy loss associated with the first peak is equal to the peak separation and the intensities of the skipping peaks decrease with increasing θ_i [19,20]. These features are clearly different from the present observation. On the other hand, the energy loss of the first peak is one half of the peak separation in the case of the subsurface channeling [18], which is also different from the present result. Moreover, the diameter of C_{60}^+(0.7 nm) is much larger than the interplanar distance (0.3 nm) in the (001) planar channel, indicating that C_{60}^+ cannot channel through the KCl crystal.

A possible origin of the observed multipeak structure is the fragmentation of C_{60}^+. When a C_{60}^+ ion impacts on a solid surface with a collision energy larger than but not far beyond the threshold energy, fragmentation of C_{60}^+ occurs via a sequential C_2-loss process. The C_2 fragments carry ~1/30 of the kinetic energy of C_{60}^+, which is in agreement with the observed peak separation. In order to examine this explanation, energy spectra were measured at different incident energies. The observed energy spectra showed similar multipeak structures and the observed peak separations were ~36 and ~69 eV at 1 and 2 keV, respectively. These values are close to 1/30 of the kinetic energies of the C_{60}^+ ions, confirming that the observed peaks correspond to the C_{60-2n}^+ ions produced by the sequential C_2-loss process. This is surprising, because the perpendicular energy for 3 keV C_{60}^+ at θ_i=1.8° is only 3 eV, which is far below the threshold energy for fragmentation reported in the previous papers [6,7], and also smaller than the activation energy for C_2 loss (~11 eV [21,22]). Nevertheless, we observed a certain amount of C_{58}^+ after grazing scattering. This will be discussed later but we first concentrate on the energy loss of the C_{60}^+ ions reflected from the surface without fragmentation.

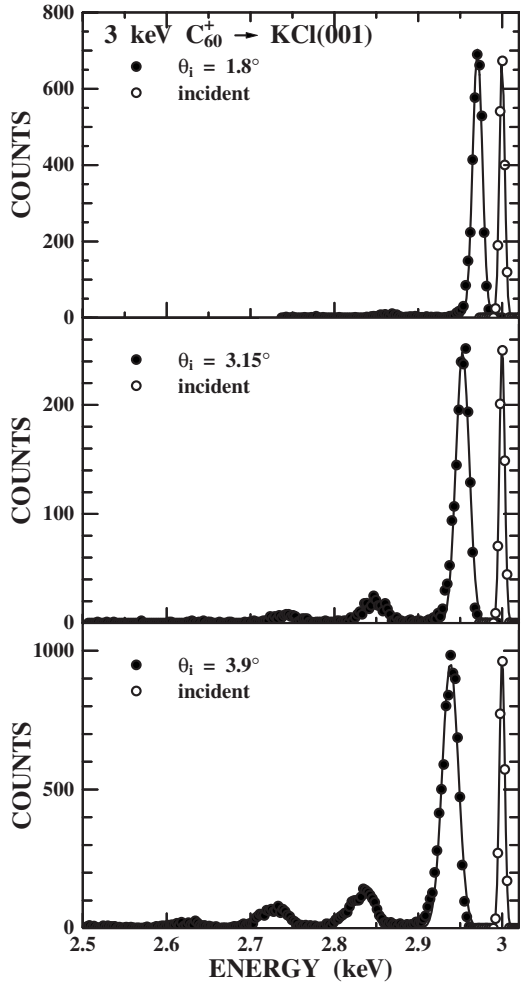

FIG. 4. Examples of the observed energy spectra of reflected ions when 3 keV C_{60}^+ ions were incident onto a KCl(001) surface under grazing incidence. A multipeak structure is clearly seen at larger θ_i.

Figure 6 shows the energy loss of the first peak as a function of θ_i. The observed energy loss is about 25 eV at θ_i

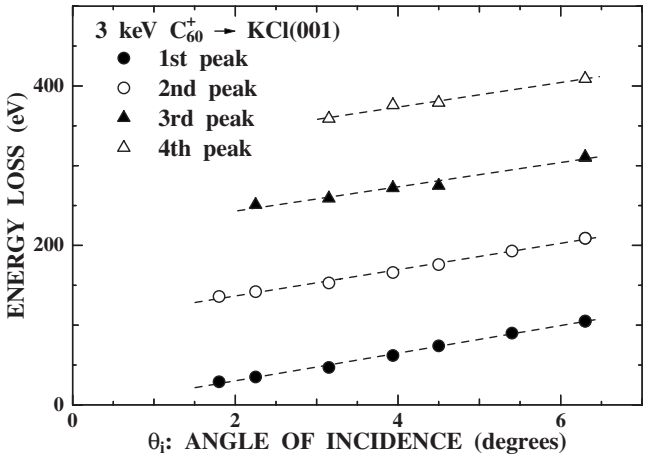

FIG. 5. Energy losses of the observed peaks in the energy spectrum for 3 keV C_{60}^+ incidence as a function of θ_i. The peak separation is almost constant (~106 eV) irrespective of θ_i. The lines through the data points guide the eye.

=1° and increases up to 100 eV at θ_i=6° for 3 keV C_{60}^+ ions. As mentioned above, the energy transfer to the surface atoms is expected to be negligibly small under the grazing scattering. Figure 7(a) shows an example of the trajectory of 3 keV C_{60}^+ ion at θ_i=1.8° calculated using the ZBL potential and the image potential. The ion is gradually deflected via a series of small angle scattering events with surface atoms. The length of the trajectory where appreciable deflection occurs is more than 8 nm in the present case [see Fig. 7(b)]. Considering the size of C_{60}^+ (0.7 nm) and the surface atomic density (~10 atoms/nm^2), more than 60 surface atoms are involved in the series of small angle scattering events in this case. The energy transfer to the surface atoms can be estimated by

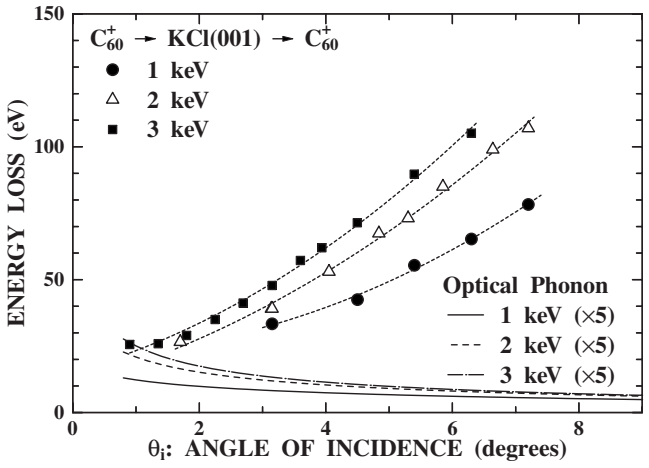

FIG. 6. Observed energy losses of 1–3 keV C_{60}^+ ions reflected from a KCl(001) surface. The calculated energy losses due to the optical phonon excitation are also shown. The lines through the data points guide the eye.

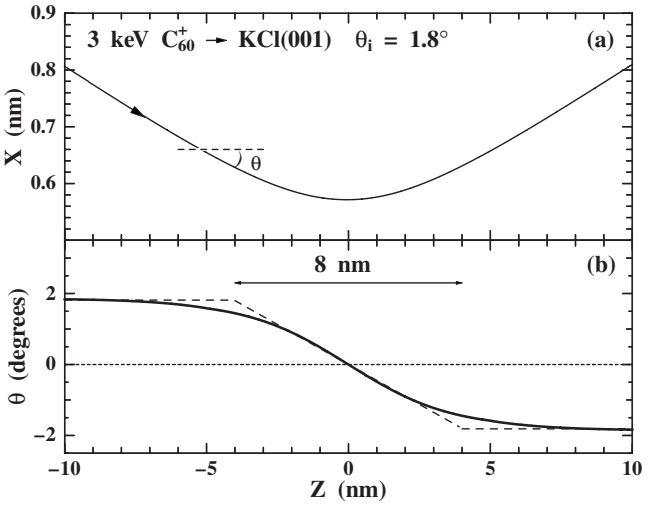

FIG. 7. A typical trajectory of 3 keV C_{60}^+ under grazing scattering from a KCl(001) surface at θ_i=1.8° (a). The change of the angle with respect to the surface plane during the reflection is also shown (b). The ion is gradually deflected by a series of small angle scattering events along the trajectory. The deflection occurs mainly in the trajectory region from z=−4 nm to z=4 nm.

$$\Delta E \approx n\frac{1}{2M_2}\left(M_1 v\frac{2\theta_i}{n}\right)^2 = \frac{4\theta_i^2 E M_1}{nM_2}, \tag{6}$$

where M_1 and M_2 are the masses of the projectile and the surface atom, respectively, E is the incident energy, and n is the number of small angle scattering events. The estimated energy loss is less than 4 eV for 3 keV C_{60}^+ at θ_i=1.8°, which is much smaller than the observed energy loss (~30 eV).

The above conclusion is also confirmed by considering a scaling law for the energy loss. Using a position-dependent stopping power, $S(x)$, the energy loss of the specularly reflected ion can be written by

$$\Delta E = \int_{-\infty}^{+\infty} S(x(z))dz = 2\int_{x_{\min}}^{\infty} S(x)\frac{dz}{dx}dx = 2v_z\int_{x_{\min}}^{\infty} S(x)\frac{1}{v_x}dx. \tag{7}$$

Note that both $x_{\min}$ and $v_x(x)$ do not depend on the ion energy if the perpendicular energy is the same. Consequently, if $S(x)$ is proportional to E^n, ΔE is proportional to $E^{n+1/2}$ at the same perpendicular energy.

During the specular reflection, the small angle scattering events with surface atoms can be well described by the impulse approximation. Thus, the momentum transfer to the surface atom is inversely proportional to the ion velocity and the energy transfer is inversely proportional to the ion energy. Consequently, the position-dependent nuclear stopping power is proportional to E^{-1}. The nuclear energy loss is, therefore, proportional to $E^{-0.5}$ if the perpendicular energy is the same. In order to examine this scaling law, the nuclear energy losses of 3 and 5 keV Ne^0 atoms reflected from LiF(001) calculated by Mertens and Winter [9] are normalized by $E^{-0.5}$ and shown as a function of the perpendicular

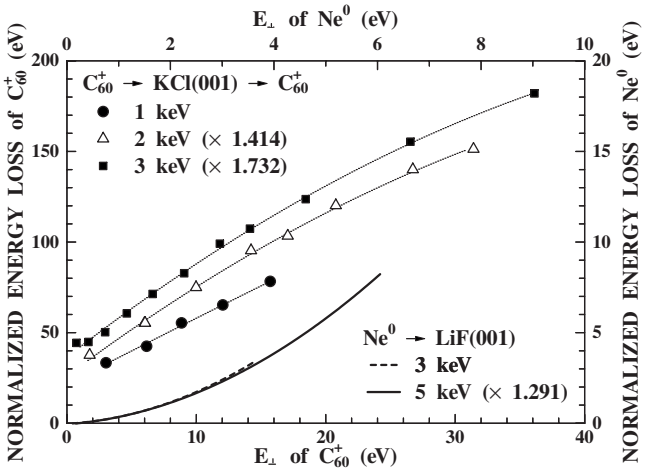

FIG. 8. Energy loss normalized by $E^{-0.5}$ as a function of the perpendicular energy. If the nuclear stopping is the dominant energy loss mechanism, all data points fall on a universal curve (see text). For comparison, the calculated nuclear energy losses for 3 and 5 keV Ne^0 reflected from LiF(001) are shown [9]. The lines through the data points guide the eye.

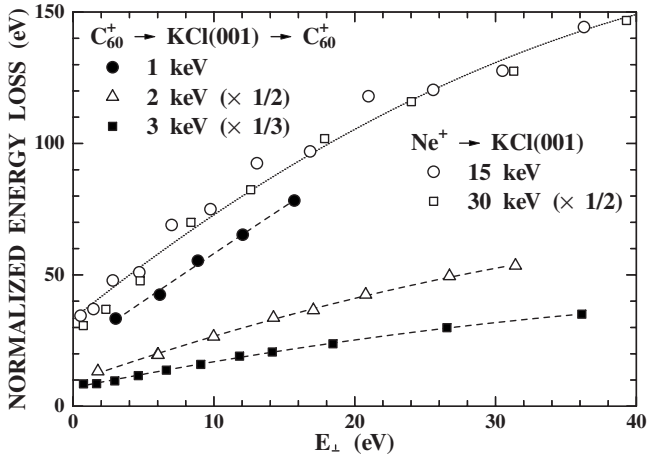

FIG. 9. Energy loss normalized by the ion energy as a function of the perpendicular energy. If the electronic stopping is the dominant energy loss mechanism, all data points fall on a universal curve (see text). For comparison, the observed energy losses for 15 and 30 keV Ne^+ ions reflected from KCl(001) are shown. The lines through the data points guide the eye.

energy in Fig. 8 (dashed and solid lines). Both energy losses fall on a universal curve after the normalization, indicating that the nuclear energy loss satisfies this scaling law. Figure 8 also shows the normalized energy losses for 1–3 keV C_{60}^+ as a function of the perpendicular energy of C_{60}^+. It is clear that the normalized energy loss does not follow the scaling law. This indicates that the observed energy loss of C_{60}^+ cannot be attributed to the nuclear stopping power.

Regarding the electronic stopping power, the direct electronic excitation is expected to be completely suppressed for slow projectiles ($v \sim 0.01$ a.u.) because of the wide band gap of KCl. The actual stopping power of insulator surfaces, however, does not vanish at velocities lower than the expected threshold velocity [23]. The stopping power was found to be proportional to the ion velocity even in the ultralow velocity regime as is similar to metal and semiconductor surfaces [23]. Therefore, the electronic energy loss should be proportional to the ion energy if the perpendicular energy is the same. Figure 9 shows the observed energy losses normalized by the ion energy as a function of the perpendicular energy. For comparison, the normalized energy losses of 15 and 30 keV Ne^+ ions specularly reflected from KCl(001) are also shown [24]. The data points of 15 and 30 keV Ne^+ ions fall on a universal curve, showing the validity of the present scaling law for the electronic energy loss. The energy losses of 1–3 keV C_{60}^+ ions, however, do not follow this scaling law. Thus, the electronic stopping power is also not responsible for the observed energy losses. In addition, our previous study showed that the charge exchange processes are almost completely suppressed for keV C_{60}^+ ions in front of a KCl(001) surface [12], indicating that there is no energy loss associated with the charge exchange processes.

Figure 10 shows the observed energy losses normalized by $E^{-0.15}$ as a function of the perpendicular energy. All data points fall on a universal curve, showing that the stopping power is proportional to $E^{-0.65}$. Although this E dependence cannot be explained by either the nuclear or the electronic stopping power alone as was discussed above, it could be reproduced by the sum of the nuclear and electronic stopping powers. In order to examine this possibility, the observed energy dependence $E^{-0.15}$ is compared with $aE+bE^{-0.5}$, which represents the sum of the nuclear and electronic energy losses. The calculated results with various a and b are shown in Fig. 11. It is clear that the observed E dependence cannot be reproduced even if both the nuclear and electronic energy losses are taken into account.

Thus, the major energy loss mechanisms are not responsible for the observed energy losses of keV C_{60}^+ ions. There is, however, another possible energy loss mechanism in the present case, namely, excitation of optical phonons [8]. The

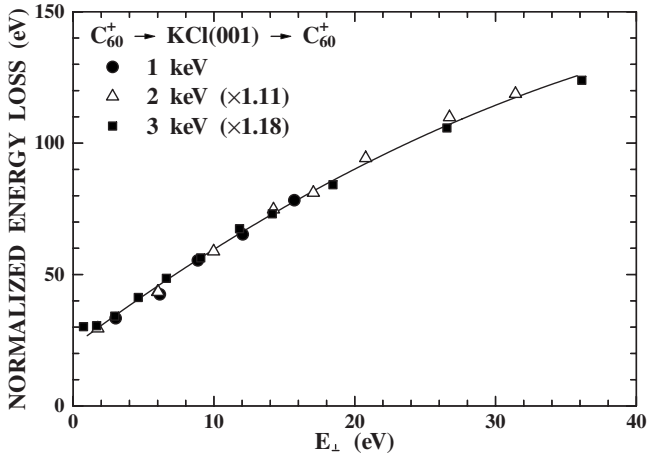

FIG. 10. Observed energy losses normalized by $E^{-0.15}$ as a function of the perpendicular energy. All data points fall on a universal curve, indicating that the stopping power is proportional to $E^{-0.65}$ (see text).

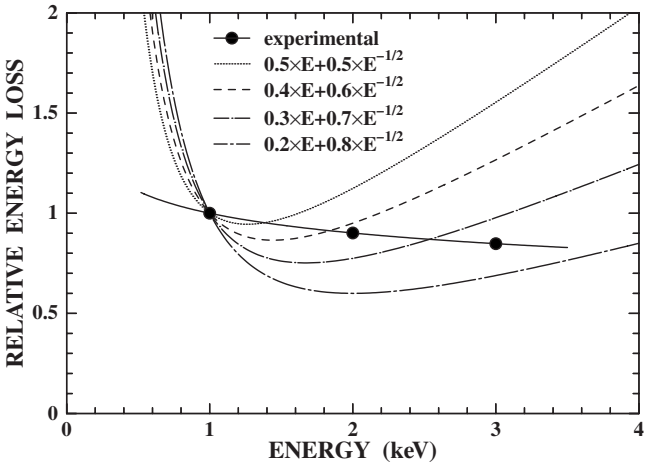

FIG. 11. Energy dependence of the relative energy loss at the same perpendicular energy. The sum of the nuclear and electronic energy losses cannot explain the observed energy dependence.

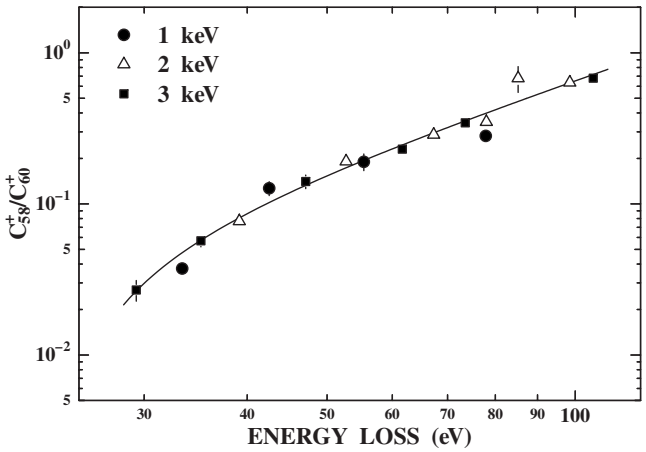

FIG. 12. Observed intensity ratios of C_{58}^+ to C_{60}^+ as a function of the energy loss of the reflected C_{60}^+. All data points fall on a universal curve irrespective of the incident energy, indicating a strong correlation between the fragmentation and the observed energy loss.

optical phonons in ionic crystals can be efficiently excited by the long range Coulomb field of the projectile ion. It was shown that the excitation of the optical phonons is the dominant energy loss mechanism for keV Ne^+ ions scattered under grazing incidence from a LiF(001) surface, where both electronic and nuclear energy losses are almost completely suppressed [8]. The contributions of the optical phonons to the observed energy losses were estimated using Eqs. (1) and (2) of Ref. [8], and the results are compared with the observed energy losses in Fig. 6. The calculation shows that the contribution of the optical phonons is negligibly small in the present case. Moreover, the calculated energy loss decreases with θ_i, while the observed energy loss increases with θ_i. Thus all the usual energy loss mechanisms cannot explain the observed energy losses.

A possible origin of the observed anomalous energy loss is related to the observed fragmentation of C_{60}^+ ions. Beck *et al.* showed that 1% of C_{60}^+ ions decay via C_2 loss when C_{60}^+ has an internal excitation energy of 38 eV [5]. In the present case, the observed C_{58}^+ fraction is 2.5% for 3 keV C_{60}^+ ions at $\theta_i = 1.8°$ and the corresponding energy loss is 29 eV. If we assume that the observed energy loss is spent for the internal excitations of C_{60}^+ ions, the present result is roughly in agreement with their result. In order to examine this explanation, the observed intensity ratio of C_{58}^+ to C_{60}^+ (this ratio is a measure of the internal excitation) is plotted as a function of the observed energy loss in Fig. 12. All data points fall on a universal curve, showing a strong correlation between the observed energy loss and the fragmentation. This indicates that the parallel component of the C_{60}^+ kinetic energy is transferred to the internal excitations, which lead to the fragmentation via C_2 loss. This scenario is also supported by the observed fact that the perpendicular energy is conserved during the grazing scattering (see Fig. 2). Only the parallel component of the kinetic energy can be responsible for the internal excitations which cause the observed fragmentation.

Now, the remaining question is the mechanism of the energy transfer from the kinetic energy to the internal excitations. Here, we note the role of the strong alternate electric field (pseudophoton field) seen by the projectile ions during grazing scattering from the surfaces of ionic crystals [25]. This alternate electric field causes the resonant coherent excitation [25,26]. The amplitude of the electric field can be as high as ~0.1 a.u. [26], which is comparable to an intense laser field. A recent theoretical study has demonstrated that an infrared ultrashort intense laser pulse (~100 fs) of $\lambda = 1800$ nm can vibrationally excite C_{60} molecules and the accumulated vibrational energy amounts to several tens eV [27]. A detailed theoretical study is required for the further quantitative explanation, which is, however, beyond the scope of the present work.

IV. CONCLUSION

We have observed anomalously large energy losses of keV C_{60}^+ ions specularly reflected from a KCl(001) surface, which cannot be explained by either nuclear stopping, electronic stopping, or the excitation of the optical phonons. A strong correlation between the observed energy loss and the fragmentation of C_{60}^+ is also observed. These results indicate that the parallel component of the kinetic energy is efficiently transferred to the internal excitation of C_{60}^+.

ACKNOWLEDGMENT

This work was supported in part by Center of Excellence for Research and Education on Complex Functional Mechanical Systems (COE program) of the Ministry of Education, Culture, Sports, Science and Technology, Japan.

[1] W. Brandt, A. Ratkowski, and R. H. Ritchie, Phys. Rev. Lett. **33**, 1325 (1974).
[2] D. S. Gemmel, J. Remillieux, J.-C. Poizat, M. J. Gaillard, R. E. Holland, and Z. Vager, Phys. Rev. Lett. **34**, 1420 (1975).
[3] Y. Susuki, M. Fritz, K. Kimura, M. Mannami, N. Sakamoto, H. Ogawa, I. Katayama, T. Noro, and H. Ikegami, Phys. Rev. A **50**, 3533 (1994).
[4] Y. Susuki, M. Fritz, K. Kimura, M. Mannami, N. Sakamoto, H. Ogawa, I. Katayama, T. Noro, and H. Ikegami, Phys. Rev. A **51**, 3868 (1995).
[5] R. D. Beck, P. St. John, M. M. Alvarez, F. Diederich, and R. L. Whetten, J. Phys. Chem. **95**, 8402 (1991).
[6] T. Fiegele, O. Echt, F. Biasiolo, C. Mair, and T. D. Märk, Chem. Phys. Lett. **316**, 387 (2000).
[7] R. T. Chancey, L. Oddershede, F. E. Harris, and J. R. Sabin, Phys. Rev. A **67**, 043203 (2003).
[8] A. G. Borisov, A. Mertens, H. Winter, and A. K. Kazansky, Phys. Rev. Lett. **83**, 5378 (1999).
[9] A. Mertens and H. Winter, Phys. Rev. Lett. **85**, 2825 (2000).
[10] M. Prutton, *Surface Physics* (Clarendon, Oxford, 1983), p. 9.
[11] K. Kimura, G. Andou, and K. Nakajima, Phys. Rev. Lett. **81**, 5438 (1998).
[12] S. Tamehiro, T. Matsushita, K. Nakajima, M. Suzuki, and K. Kimura, Nucl. Instrum. Methods Phys. Res. B **256**, 16 (2007).
[13] S. Wethekam, H. Winter, H. Cederquist, and H. Zettergren, Phys. Rev. Lett. **99**, 037601 (2007).
[14] M. Hillenkamp, J. Pfister, M. M. Kappes, and R. P. Webb, J. Chem. Phys. **111**, 10303 (1999).
[15] H. Winter, C. Auth, R. Schuch, and E. Beebe, Phys. Rev. Lett. **71**, 1939 (1993).
[16] H. Zettergren, H. T. Schmidt, H. Cederquist, J. Jensen, S. Tomita, P. Hvelplund, H. Lebius, and B. A. Huber, Phys. Rev. A **66**, 032710 (2002).
[17] Y. H. Ohtsuki, K. Koyama, and Y. Yamamura, Phys. Rev. B **20**, 5044 (1979).
[18] K. Kimura, M. Hasegawa, and M. H. Mannami, Phys. Rev. B **36**, 7 (1987).
[19] F. Stoelzle and R. Pfandzelter, Phys. Lett. A **150**, 315 (1990).
[20] K. Narumi, Y. Fujii, K. Kimura, M. Mannami, and H. Hara, Surf. Sci. **303**, 187 (1994).
[21] A. D. Boese and G. E. Scuseria, Chem. Phys. Lett. **294**, 233 (1998).
[22] S. Tomita, J. U. Andersen, C. Gottrup, P. Hvelplund, and U. V. Pedersen, Phys. Rev. Lett. **87**, 073401 (2001).
[23] J. I. Juaristi, C. Auth, H. Winter, A. Arnau, K. Eder, D. Semrad, F. Aumayr, P. Bauer, and P. M. Echenique, Phys. Rev. Lett. **84**, 2124 (2000).
[24] K. Nakajima, S. Sonobe, and K. Kimura, Nucl. Instrum. Methods Phys. Res. B **164/165**, 553 (2000).
[25] C. Auth, A. Mertens, H. Winter, A. G. Borisov, and F. J. Garcia de Abajo, Phys. Rev. Lett. **79**, 4477 (1997).
[26] C. Auth and H. Winter, Phys. Rev. A **62**, 012903 (2000).
[27] R. Sahnoun, K. Nakai, Y. Sato, H. Kono, Y. Fujimura, and M. Tanaka, J. Chem. Phys. **125**, 184306 (2006).